https://doi.org/10.5194/egusphere-2026-850
Preprint. Discussion started: 17 February 2026

Quantifying Compounded Economic Impacts and Disease Burden of Flooding in Can Tho, Vietnam

Yamile Villafani[1,2], Heiko Apel[1], Laurens J.N. Oostwegel[1], Thi Thao Nguyen Huynh[3,4,5], Hong Quan Nguyen[5,6], Nigel K. Downes[7], Andrea Cominola[8,9], and Nivedita Sairam[1,*]

[1] GFZ German Research Centre for Geosciences, Hydrology, Potsdam, Germany
[2] Geography Department, Humboldt-Universität zu Berlin, Berlin, Germany
[3] IHE Delft Institute for Water Education, Delft, The Netherlands
[4] Faculty of Civil Engineering and Geosciences, Delft University of Technology, Delft, The Netherlands
[5] Institute for Environment and Resources, Vietnam National University, Ho Chi Minh City, Vietnam
[6] Institute for Circular Economy Development, Vietnam National University, Ho Chi Minh City, Vietnam
[7] College of Environment and Natural Resources, Can Tho University, Can Tho 92000, Vietnam
[8] Chair of Digital Water Systems, Technische Universität Berlin, Straße des 17. Juni 135, Berlin, 10623, Germany
[9] Einstein Center Digital Future, Robert-Koch-Forum, Wilhelmstraße 67, Berlin, 10117, Germany

Correspondence to: Nivedita Sairam (nivedita@gfz.de)

Abstract. In growing urban areas, floods increasingly threaten daily life, causing economic losses and raising public health burdens through microbial exposure. Yet, risk assessments often treat economic and health impacts separately, overlooking their interconnected nature and potentially biasing adaptation strategies. This study addresses this gap by quantifying spatial and distributional disparities in flood risks across economic and health dimensions in Can Tho City, a flood-prone urban area in Vietnam's Mekong Delta.

We calibrate flood impact models for the economic sector by estimating residential building losses, and for the health sector by predicting rotavirus A and *E. coli* concentrations in floodwaters and resulting disease burden. By combining probabilistic flood simulations with exposure data, we develop a multi-risk framework to capture co-occurring economic and health impacts. Economic risk is quantified via Value at Risk (VaR) and Expected Annual Damage (EAD) for fluvial–pluvial flooding, while health risk is expressed through the Population Health at Risk (PHaR) and Expected Annual Cases (EAC).

Results show pronounced spatial disparities in intersecting risks. The highest combined economic and health risks are found in Phu Thu and Thuong Thanh wards (Cai Rang district) and An Binh ward (Ninh Kieu district), while An Hoi, An Lac, and Tan An wards (Ninh Kieu district) experience consistently low risks. These findings highlight how urbanization and flooding interact to shape multi-sector vulnerabilities in delta cities.

1 Introduction

Floods are among the most damaging disasters globally, with their impacts intensifying under changing climatic and societal conditions. The frequency and intensity of flood events are expected to increase, largely driven by climate change, which alters

https://doi.org/10.5194/egusphere-2026-850
Preprint. Discussion started: 17 February 2026

precipitation patterns and amplifies extreme events (IPCC, 2022). Urbanisation and population growth often lead to higher exposure to floods, thereby exacerbating flood risks (Tellman et al., 2021). Exposure of large numbers of people and assets to flooding leads to widespread infrastructure impacts, severe economic consequences, and a burden on human health. Flood-related health burden may arise from exposure to contaminated water, physical hazards, and disrupted living conditions, increasing the risk of infectious disease, injury, and longer-term adverse health outcomes.

The IPCC risk framework provides a comprehensive approach to analysing flood risk as a product of the dynamic interactions of hazard, vulnerability, and exposure (IPCC, 2012). The hazard component refers to the physical process and events, such as extreme precipitation, storm surges, tropical cyclones, which can lead to flooding. Exposure captures the presence of physical assets and people in flood-prone areas, increased by population growth and urban sprawl. Vulnerability is defined as the degree of potential adverse effect on the human or ecological systems (Kron, 2005). The changing patterns of hazard, vulnerability, and exposure are major contributors to increased losses, stressing the importance of understanding the nature of these components for the development of effective adaptation and disaster risk management strategies (Climate and Development Knowledge Network, 2012).

Flood impacts include adverse consequences that lie beyond the limits of mitigation and adaptation, encompassing both irreversible loss and reparable damage (Bouwer, 2019). They are commonly analysed in economic and non-economic terms. Economic losses are defined as the loss of resources, goods, and services commonly traded in markets. Conversely, non-economic losses include loss of ecosystems and social losses, among others (Van Der Geest et al., 2019). Also characterised as direct and indirect losses, direct losses include the loss of human life, damage to infrastructure, and business interruption, while indirect losses are associated with, for example, changes in long-term wellbeing and development. These latter impacts are harder to estimate and, thus, remain usually underreported (UNFCCC, 2012).

Economic losses from flood events to assets have widely been studied, with recent research resulting in various models that capture their related losses. These models range from traditional depth–damage functions, which link flood water depth to monetary loss, to more advanced probabilistic and multivariate approaches that incorporate exposure and vulnerability factors (Merz et al., 2010; Jongman et al., 2012). In Southeast Asia (SEA), an area where flooding poses substantial risks, region-specific flood loss models are increasingly being developed. For example, flood depth–damage functions and the incorporation of additional variables (e.g., flood duration and velocity) have been developed to assess losses related to property and household impacts (D'Ayala et al., 2020; Romali & Yusop, 2021), losses to the agricultural sector and productivity (Shrestha et al., 2024; Win et al., 2018), and the disruption of industrial facilities and commercial activity (Darnkachatarn & Kajitani, 2025). Despite these advances, most applications remain centred on losses related to economic sectors, while the social and health dimensions remain underrepresented in flood loss modelling.

The predominant focus on economic losses and limited consideration of social and health dimensions of flood impacts reveal a critical gap in flood risk assessment, as existing models are poorly equipped to capture the evolving and multidimensional impacts of flooding in rapidly urbanising environments. This is the case of the Vietnamese Mekong Delta (VMD), an area which experiences recurrent and severe flooding driven by climatic and socio-ecological factors. Low elevation, dense

https://doi.org/10.5194/egusphere-2026-850
Preprint. Discussion started: 17 February 2026

population, and rapid urban expansion make the region highly susceptible to fluvial and pluvial floods intensified by sea-level rise and tropical cyclones (Tran et al., 2022; Olcese et al., 2024). Can Tho City, the largest city in the region that is located in the central part of the delta, represents an example of increased flood vulnerability. Recurrent compound floodings have caused substantial economic losses and infrastructure impacts, with annual flood losses estimated at US$4.3 million (UNU-EHS, 2021). Major events, such as the 2011 floods, resulted in direct losses exceeding US$11 million (Chinh et al., 2016).

In response, subsequent studies have sought to quantify economic losses in Can Tho by applying multivariate statistical approaches to the 2011 flood event to assess impacts on households and small businesses (Chinh et al., 2016). Such studies identified flood loss drivers and quantified their effects, informing subsequent improvements in flood loss modelling for residential buildings and household contents (Chinh et al., 2017). However, despite incorporating multiple loss determinants, these models remain deterministic and do not allow for the quantification of uncertainties. One of the first probabilistic flood loss models in Vietnam was a Bayesian Network model for micro-businesses in Ho Chi Minh City, which was then transferred to Can Tho as a test case study (Buch et al., 2025). The predictive performance of the Bayesian Network model was, however, limited, reflecting the complexity in flood damage processes in shophouse contents and business interruption.

Beyond economic losses, floods result in diverse public health risks, particularly where inadequate water and sanitation infrastructure intensifies exposure to contaminated floodwater. The water supply, sewage, and drainage systems in Can Tho face challenges related to insufficient water drainage, pollution, and incomplete sewer coverage. Although the city has focused on improving its water infrastructure to achieve a better water quality and interconnection to the drainage networks, flood-induced sewer overflows and wastewater discharge into public sources remain a key challenge (Cantho Water Supply, 2024). Microbial pathogens present in flood and sewer water pose risks to human health related to waterborne diseases, including diarrhoea, continuing to be a major cause of illness and death among children. Notably, rotavirus is the most detected pathogen in Vietnam, followed by other pathogens such as norovirus, *Shigella*, and *Salmonella* (Anders et al., 2015).

The health risks associated with rotavirus A and *Escherichia coli* (*E. coli*) have been studied for the city of Can Tho using Quantitative Microbial Risk Assessment (QMRA) approaches (Haas et al., 2014). QMRA provides a structured framework to estimate infection probabilities and disease burden resulting from the exposure to pathogens, integrating exposure pathways and dose-response relationships. Studies using this approach include Nguyen et al. (2017), who quantified concentrations of *E. coli* and *Salmonella* following a flooding event, reporting levels exceeding the limits established in water standards. Likewise, Huynh et al. (2019) documented the prevalence of rotavirus A and *E. coli* in floodwater, noting that contamination levels were nearly equivalent to those measured in sewer water. More recently, Huynh et al. (2024) quantified the health impacts and disease burden associated with rotavirus A and linked it to urban traffic exposure, identifying motorcyclists as the most exposed population group. Such quantitative assessments of flood impacts to economic and health sectors have been conducted separately across spatially and temporally heterogeneous contexts. Integrating economic flood loss models with

https://doi.org/10.5194/egusphere-2026-850
Preprint. Discussion started: 17 February 2026

QMRA-based health risk assessments offers a pathway towards comprehensive flood risk assessment and management across economic and health sectors, with a particular focus on co-occurrence of economic and health burden.

The objective of this study is two-fold. First, we aim to calibrate flood impact prediction models for the economic sector by predicting building losses to the residential buildings and for the health-sector by predicting contamination-levels of pathogens in flood waters and the subsequent consequences on human health. Second, we aim to elucidate the co-occurrence of economic losses and disease burden by integrating spatially explicit quantifications of economic losses with the health burden caused by exposure to rotavirus A and *E. coli*. This multi-sector focus allows for a comprehensive assessment of built-environment and public health vulnerabilities. To this end, we calibrate and validate a state-of-the-art Bayesian Regression Model for flood loss estimation in private households and implement QMRA considering rotavirus A and *E. coli* contamination in flood waters. We integrate the developed economic and health impact models with probabilistic flood hazard maps with different return periods and population and building exposure datasets.

The manuscript is structured as follows: Section 2 describes the data and methods, starting with the description of the study area, followed by the description of the impact models developed for residential building losses and health outcomes, as well as the components of the flood risk and the associated metrics. Section 3 presents the results and discussions, while Section 4 concludes with the main findings.

2 Data and Methods

2.1. Study area

Can Tho City, located on the western bank of the Hau River, a major branch of the Mekong River in the delta, serves as a key economic hub in the region, while facing challenges related to urban growth and climate change. In 2024, the city's population reached a total of 1,271,723 across four rural and five urban districts (Can Tho City Statistics Office, 2025). The annual flood season extends from July to December, undergoing both pluvial and fluvial floodings. Pluvial flooding results from intense rainfall overwhelming the drainage networks. Fluvial flooding, on the other hand, occurs when the Hau River overflows, influenced by high tides and upstream flows (Huynh et al., 2024).

https://doi.org/10.5194/egusphere-2026-850
Preprint. Discussion started: 17 February 2026

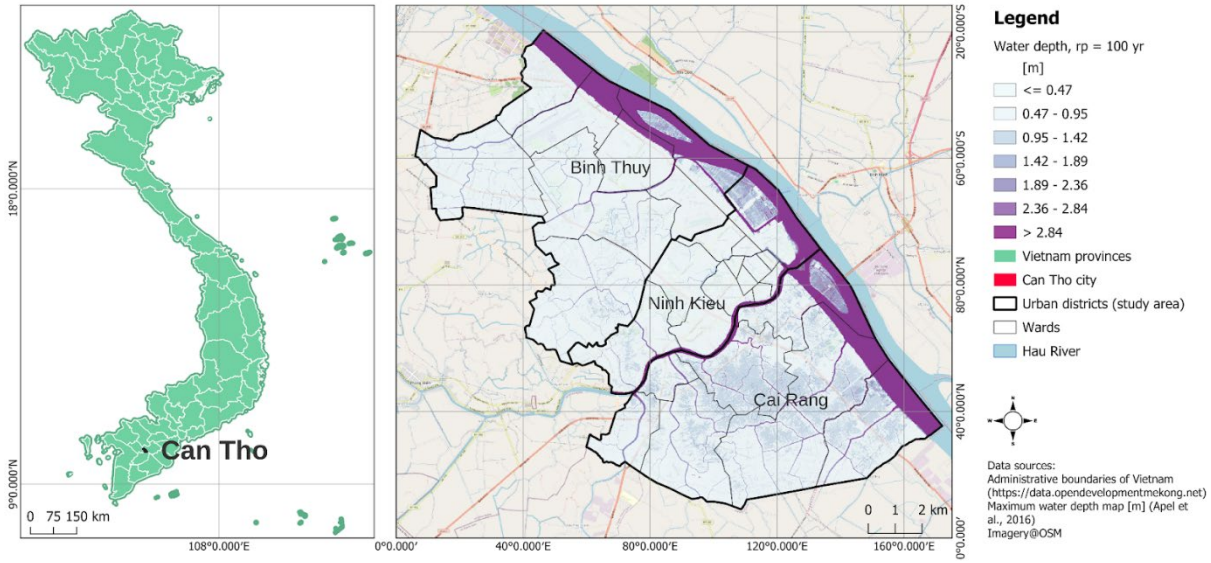

Figure 1. Maps representing the location of Can Tho in Vietnam (left) and the flood inundation map of the three urban districts of Binh Thuy, Ninh Kieu, and Cai Rang in the study area of Can Tho (right).

Our study focuses on three urban districts: Binh Thuy in the northern part of the city, Ninh Kieu in the city centre, and Cai Rang in the southern part of Can Tho (Figure 1, map on the right-hand side). As of 2024, Cai Rang is the least populated urban district in the city (109,319), followed by Binh Thuy (151,834), while Ninh Kieu (299,584) hosts nearly double the population of Binh Thuy, corresponding to a population density 2.33 times higher than the city average (Can Tho City Statistics Office, 2024). As the region's economic centre, the city is undergoing rapid urban expansion, with development spreading southwards into formerly rural districts. Residents living along rivers and canals consequently face heightened exposure to flood risk. In addition to flooding, the city has increasingly faced other recurrent challenges, including heatwaves, infectious diseases, and environmental pollution (Resilient Cities Network et al., 2024).

2.2. Flood impact models

In this section, we describe the underlying data and methodology involved in the development of the impact models for predicting economic losses, that is, residential building losses, and disease burden, from contamination levels of *E. Coli* and rotavirus A in flood waters. The calibration of the models is based on empirical survey data (section 2.2.1) and water quality samples (section 2.2.2). The models are evaluated using the performance metrics described in section 2.2.3.

2.2.1. Modelling residential building losses

Flood loss models for residential buildings in Can Tho were developed based on an empirical dataset (n = 480 private households) obtained from interviews conducted following the 2011 flood event (see, Chinh et al., 2015 for details on the survey) (see Figure 2). We express the impacts associated with residential buildings as relative building losses (*rbloss*), defined

https://doi.org/10.5194/egusphere-2026-850
Preprint. Discussion started: 17 February 2026

as the ratio of repair cost to the total reconstruction cost of the building. The *rbloss* values range between 0 and 1, representing no loss and total loss, respectively. In our survey, the reported relative losses range between 0.00% and 97.22%, with predominantly low-to-moderate loss levels, with the distribution skewed toward lower losses (see Supplement Material, Data description S1).

We advance the flood loss models for Can Tho presented in Chinh et al. (2016) by developing Bayesian regression models using zero-one inflated beta distributions. This approach, following Schoppa et al. (2020), is well suited to relative loss data bounded between 0 and 1, and explicitly captures frequent occurrences of 0 (no loss) and 1 (total loss) (see Figure 2 for an example distribution). These models are designed to represent not only the central tendency of losses but also the associated uncertainty in the loss estimation, accounting for the shape and spread of the loss distribution. The cumulative distribution function (CDF) in Equation 1 is used.

$$BEINF(y \mid \lambda, \mu, \phi) = \lambda + (1 - \lambda) \cdot F_{Beta}(y \mid \mu, \phi) \quad (1)$$

where y is the observed relative loss (response variable), λ is the zero-one inflation probability observation of 0 and 1 responses, and $F_{Beta}(y \mid \mu, \phi)$ refers to the cumulative beta distribution with mean (μ) and precision (ϕ) parameters. The Bayesian regression structure for the model parameters is defined in Equation 2 (a-d).

$$\boldsymbol{Y_i = BEINF(\lambda, \mu_i, \phi)} \quad (2a)$$

$$\boldsymbol{logit(\mu_i) = \alpha_\mu + \beta_{\mu,} X_{\mu,i}} \quad (2b)$$

$$\boldsymbol{logit(\ \ ) = \alpha_\lambda} \quad (2c)$$

$$\boldsymbol{log(\phi) = \alpha_\phi} \quad (2d)$$

These define the relationship between the distribution parameters and their predictors for each observation $\boldsymbol{i}$. Here, $\boldsymbol{\alpha}$ denotes the intercept, and $\boldsymbol{\beta}$ corresponds to the slope coefficients associated with the predictors of loss $\boldsymbol{X}$. The mean parameter ($\boldsymbol{\mu}$) is the expected value of the relative loss, the precision parameter ($\boldsymbol{\phi}$) captures the dispersion of losses around the mean, and the inflation parameter ($\boldsymbol{\lambda}$) determines the probability of observing total or no loss. These last two parameters remain constant across all observations, specified as intercept functions (see equations 2c and 2d). This accounts for excess zeros and variability in positive losses, with all observed variation explained by the mean parameter.

We estimate the mean $\boldsymbol{\mu}$ from a subset of available candidate predictors of relative flood loss to residential households (*rbloss*) at the city-wide scale for application, as described in Chinh *et al.* (2016). The subset included water depth (*wd*), duration of the flood event (*dur*), frequency of past flood events experienced (*f_events*), and building value (*bv*). We compare the candidate multivariable model ($\boldsymbol{m_1}$, eq. 3) to parsimonious models ($\boldsymbol{m_2}$, eq. 4; $\boldsymbol{m_3}$, eq. 5) by reducing the number of predictors, one at a time (Mohor *et al.*, 2021) in the order of importance from Chinh et al. (2015) (see Supplementary Material, Bayesian Regression Models S2):

$$\boldsymbol{m_1: logit(\mu_i) = \alpha_\mu + \beta_{\mu,1}\, wd_i + \beta_{\mu,2}\, dur_i + \beta_{\mu,3}\, f\_events_i + \beta_{\mu,4}\, bv_i,} \quad (3)$$

$$\boldsymbol{m_2: logit(\mu_i) = \alpha_\mu + \beta_{\mu,1}\, wd_i + \beta_{\mu,2}\, bv_i,} \quad (4)$$

$$\boldsymbol{m_3: logit(\mu_i) = \alpha_\mu} \quad (5)$$

https://doi.org/10.5194/egusphere-2026-850
Preprint. Discussion started: 17 February 2026

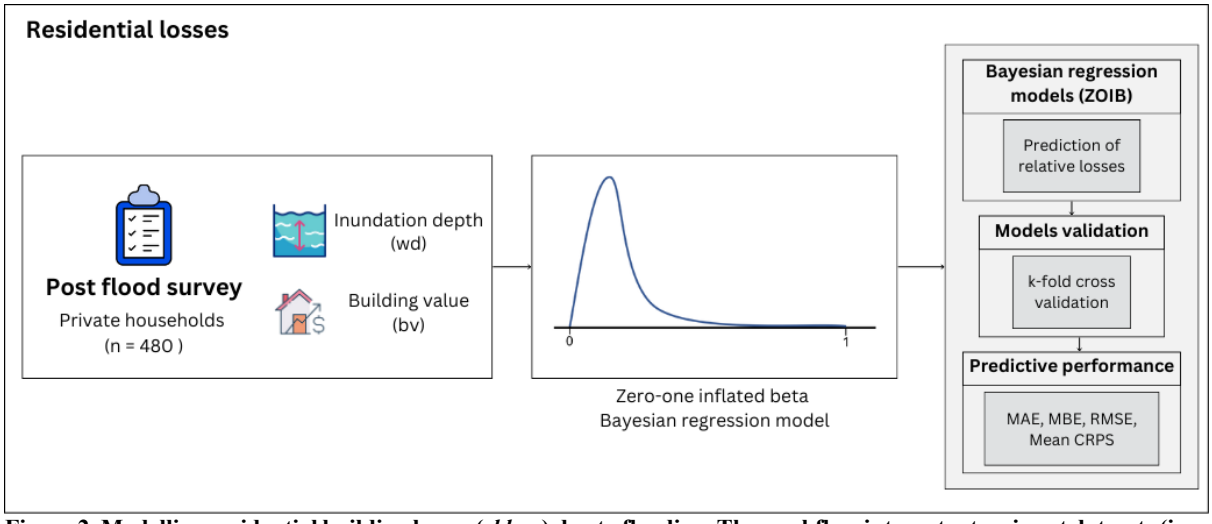

Figure 2. Modelling residential building losses (*rbloss*) due to flooding. The workflow integrates two input datasets (inundation depth and building value) to model flood-related residential building losses which are validated using k-fold cross-validation.

2.2.2. Modelling pathogen concentration in flood waters

Disease burden derived from infections related to rotavirus A and *E. coli* are modelled based on water quality sampling points obtained from sewage, surface, and flooded water after the 2016 flood in Can Tho (n = 30) (see, Nguyen *et al.*, 2017 for details on the dataset) (see Figure 3). The dataset covers the water depth and microbial parameters, such as the pathogen concentrations. These serve as calibration data for the concentrations ($\boldsymbol{c}$) predictions of rotavirus A (gc/mL, genome copies per millimetre) and *E. coli* (CFU/mL, Colony Forming Units per millimetre). The distributions are left-skewed, with *E. coli* concentrations clustered between 0.00 and 8.99×10^{3} CFU/mL, while rotavirus A is detected at concentrations ranging 0.00–2.96×10^{6} gc/mL (see Supplement Material, Data description S1).

We build candidate models to simulate pathogen concentrations. First, we choose the appropriate response distribution from (1) an intercept-only negative binomial model, suitable for overdispersed data where the variance exceeds the mean (see equation 6a). This is commonly observed in microbial studies with many zero-observations (Lloyd-Smith, 2007; Yirga *et al.*, 2020). (2) An intercept-only hurdle lognormal model that separates the zeros and positive values (see equation 6b), used for semi-continuous data where a substantial proportion of samples are below detection limits, and positive measurements are highly skewed, often used in microbiology (Gonzales-Barron et al., 2010; Lison et al., 2024).

$$\boldsymbol{F(y) = F_{NegBinomial}(y \mid \mu, \sigma)} \quad (6a)$$

$$\boldsymbol{F(y) = \pi + (1 - \pi)\, F_{LogNormal}(y \mid \mu, \sigma)} \quad (6b)$$

where $\boldsymbol{\mu}$ represents the mean of the distributions. The overall probability of zero counts is $\boldsymbol{\pi}$, and $\boldsymbol{\sigma}$ is the standard deviation, with both parameters remaining constant for all observations. We compare these models, where $\boldsymbol{\alpha}$ the intercept of the models,

https://doi.org/10.5194/egusphere-2026-850
Preprint. Discussion started: 17 February 2026

and $\boldsymbol{\beta}$ the slopes for the $\boldsymbol{i}$ observations. We estimate the mean using several combinations of predictors against the simplest intercept-only model.

The first candidate model ($\boldsymbol{r_{nb1}}$, eq. 7) is an intercept-only negative binomial regression, similar to the case for the third model ($\boldsymbol{r_{hl1}}$, eq. 9a, b), a hurdle lognormal model. The second and fourth models ($\boldsymbol{r_{nb2}}$, eq. 8; $\boldsymbol{r_{hl2}}$, eq. 10a, b) integrate additional predictors in the negative binomial and hurdle lognormal regression models. The predictors include water depth (*wd*), median topographic slope (*topo*), diameter of the closest sewer (*sewer*), and the inverse distance to the closest sewer (*inv_d*). We selected these variables based on previous studies highlighting drivers of pathogenic presence in floodwaters. Probable contamination sources may originate from septic tanks of local households near rivers or canals (Huynh et al., 2019). During flooding, elevated water levels can connect these contaminated sources to surface water, increasing the risk of pathogen presence.

$$\boldsymbol{r_{nb1}}: \boldsymbol{log(\mu_i) = \alpha_\mu} \tag{7}$$

$$\boldsymbol{r_{nb2}}: \boldsymbol{log(\mu_i) = \alpha_\mu + \beta_{\mu,1}\, wd_i + \beta_{\mu,2}\, topo_i + \beta_{\mu,3}\, sewer_i + \beta_{\mu,4}\, inv\_d_i} \tag{8}$$

$$\boldsymbol{r_{hl1}}: \boldsymbol{logit(\pi) = \alpha_\pi}, \tag{9a}$$

$$\boldsymbol{log(\mu) = \alpha_\mu} \tag{9b}$$

$$\boldsymbol{r_{hl2}}: \boldsymbol{logit(\pi_i) = \alpha_\pi + \beta_{\pi,1}\, wd_i + \beta_{\pi,2}\, topo_i + \beta_{\pi,3}\, sewer_i + \beta_{\pi,4}\, inv\_d_i}, \tag{10a}$$

$$\boldsymbol{log(\mu_i) = \alpha_\mu + \beta_{\mu,1}\, wd_i + \beta_{\mu,2}\, topo_i + \beta_{\mu,3}\, sewer_i + \beta_{\mu,4}\, inv\_d_i} \tag{10b}$$

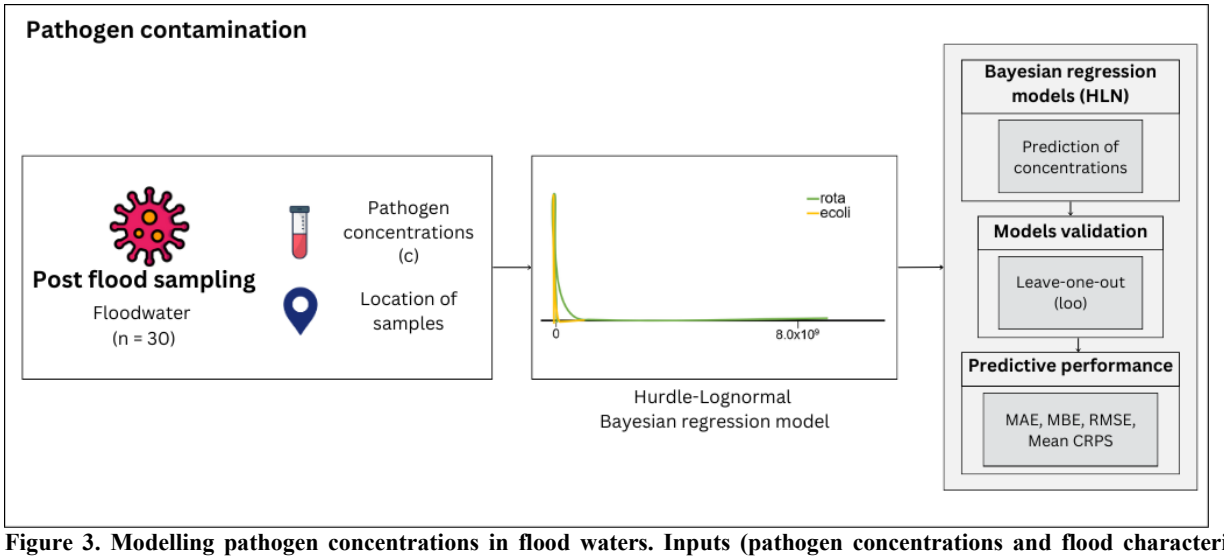

Figure 3. Modelling pathogen concentrations in flood waters. Inputs (pathogen concentrations and flood characteristics at the location of samples) were integrated to predict concentrations of rotavirus A and *E. coli* in flood waters. Models are trained and validated using leave-one-out (LOO) cross-validation.

https://doi.org/10.5194/egusphere-2026-850
Preprint. Discussion started: 17 February 2026

2.2.3. Predictive performance assessment:

The models for predicting building losses and contamination levels undergo a performance evaluation using the expected log-pointwise predictive density (ELPD) (eq. 11) to comparatively analyse the formulated models based on their predictive performance and select the best performing one (see Supplementary Material, Bayesian Regression Models S2.1). The ELPD is formulated as:

$$\boldsymbol{ELPD} = \sum_{i=1}^{n} \boldsymbol{log}\, \boldsymbol{p}(\boldsymbol{y_i}|\boldsymbol{D_{-i}}) \quad (11)$$

where $\boldsymbol{y_i}$ is the observed value for observation $\boldsymbol{i}$, $\boldsymbol{D_{-i}}$ represents the data excluding $\boldsymbol{i}$, and $\boldsymbol{p}(\boldsymbol{y_i}|\boldsymbol{D_{-i}})$ is the posterior predictive density. Higher values indicate higher predictive performance.

Following the selection of the best performing model based on the ELPD, we employ k-fold cross-validation and the Leave-One-Out (LOO) method to assess the accuracy of the building loss and pathogen concentration models, respectively. Model performance of each model is computed using the following metrics: Mean Absolute Error (*MAE*), Root Mean Squared Error (*RMSE*), Mean Bias Error (*MBE*), and Mean Continuous Ranked Probability Score (*MEAN CRPS*) (see Supplementary Material, Metrics for predictive performance evaluation S2.2).

2.3. Assessing multi-risks of flooding

We integrate the hazard, exposure, and vulnerability components to quantify economic risk and disease burden. In this section, we describe the details of the developed multi-risk assessment framework including flood hazard simulation, building and population exposure datasets, QMRA and the integration of flood impact models developed in Section 2.2. This framework provides key risk metrics: the Value at Risk (VaR), Population Health at Risk (PHaR), Estimated Annual Damage (EAD) and

https://doi.org/10.5194/egusphere-2026-850
Preprint. Discussion started: 17 February 2026

the Expected Annual Cases (EAC). The following subsections describe the specific inputs associated with each component of flood risk, as summarised in Figure 4.

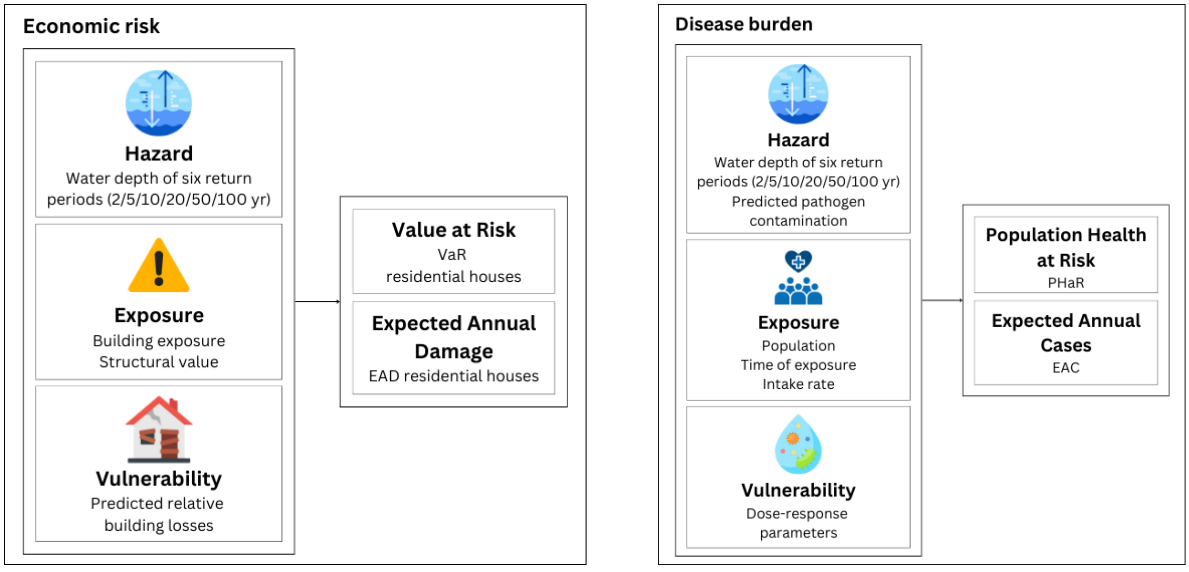

Figure 4. Multi-risk assessment framework including economic risk to residential buildings (left), and disease burden related to pathogens (right).

2.3.1. Flood Hazard Simulations

The inundation simulations for different return periods and the derivation of the associated boundary conditions are based on the probabilistic fluvial-pluvial flood hazard analysis presented in Apel et al. (2016), but extended to cover the three districts of this study. Moreover, the spatial resolution was refined to 5 m. Due to the substantially longer simulation times required for the much larger simulation area and finer spatial resolution, the simulations did not cover the full probabilistic set of scenarios, but only the most likely hazard scenarios were considered for the selected return periods rp = 2, 5, 10, 20, 50, and 100 years. The hazard analysis comprises the analysis of fluvial flood hazard, pluvial flood hazard, combined fluvial-pluvial flood hazard, and tidal flood hazard. Details about the hazard analysis are given in the following sections.

For the fluvial flood simulations, the boundary conditions along the Hau and Can Tho rivers were derived using bivariate extreme value statistics for flood peak discharge Qp and flood volume V at Kratie, the apex of the Mekong delta, published by Dung et al. (2015). With these Qp-V-pairs synthetic flood hydrographs were generated and flood simulations were performed by the large scale quasi-2D model of the Mekong delta (Dung et al., 2011), thereby generating the hydraulic boundary conditions in terms of water levels for the fluvial flood hazard simulations in Can Tho.

The pluvial flood input, *i.e.*, the rainfall intensities are based on extreme value statistics of the gauge Can Tho airport, as reported in Apel et al. (2016). Unfortunately, no information about spatial extent and spatial and temporal intensity of the typically convective rainstorm during the monsoon season in the Mekong delta are available. Therefore, we relied on the

https://doi.org/10.5194/egusphere-2026-850
Preprint. Discussion started: 17 February 2026

following simplifying assumptions: spatially uniform rainfall distribution and uniform temporal distribution over a reference rainfall duration of 90 minutes. These assumptions are simplifications of the actual rainfall dynamics, but used as standards in hydraulic design of, *e.g.*, sewer systems (Apel et al., 2024). For the hydraulic simulation the 2D raster-based hydraulic model RIM2D was used (Apel et al., 2022).

Inundation depths below 0.05 m are classified as no inundation, as households exposed to such shallow flooding reported no loss (Chinh et al., 2016, 2017). This threshold is applied to determine building exposure and the affected population within the city. In this study, we utilise the hazard maps representing present climate conditions under the combined fluvial–pluvial flood scenarios. Considering the extreme 100-year return period scenario, the highest return period analysed in this study, inundation depths (*wd*) ranged between 0.28–1.154 m (interquartile range), with a median of 0.553 m.

2.3.2. Exposure Data (Buildings, Population):

We estimate exposure data for private households using the Global Dynamic Exposure Model (GDE, Schorlemmer et al., 2026) by combining data about individual buildings from the OpenBuildingMap dataset, such as the location, occupancy type and height (Oostwegel et al., 2025), with district-level information from the Global Exposure Model (Yepes-Estrada et al., 2023). The exposure dataset includes information on building use, replacement costs, and structural type, allowing for a differentiation based on building type (residential, commercial, and industrial structures) and a quantification of monetary losses. Residential buildings located in areas where water depth (*wd*) exceeds 0.05 m were considered in the exposure analysis. Structural values were assigned based on building typologies and assets. Considering the extreme 100-year return period scenario, the structural values of residential buildings exposed to flooding over the threshold ranged between 778.54–3,115.74 US$, with a median at 1,575.26 US$.

The population was obtained from the Can Tho City Statistics Office (2018). The statistical yearbook provides population data for the city of Can Tho, disaggregated by district and ward. The estimation for exposed population was derived by combining building exposure data with the proportion of areas experiencing water depths greater than the indicated threshold. We used vulnerable populations, that is, only a portion of the whole population, namely children below 5 years old and seniors above 65 years old (data obtained from GSO, 2020).

2.3.3. Quantitative Microbial Risk Assessment (QMRA)

Disease burden associated with pathogen infections are modelled using the Quantitative Microbial Risk Assessment (QMRA) framework. This approach comprises four stages: hazard identification, exposure assessment, dose-response assessment, and risk characterisation to estimate the risk of infection from microbial contaminants (Haas et al., 2014). The pathogens considered in this study are rotavirus A and *Escherichia coli* (*E. coli*), both known to cause diarrhoeal diseases. Exposure to these pathogens is assumed to occur through accidental ingestion of floodwater, with ingestion rates differentiated for adults and children.

https://doi.org/10.5194/egusphere-2026-850
Preprint. Discussion started: 17 February 2026

The intake dose (μ) for each pathogen is estimated as a function of the pathogen concentration (c), the ingested volume of water (IR), and the duration of exposure (t_e), as defined by Haas et al. (2014) (see, eq. 12):

$$\mu = c \times IR \times t_e \quad (12)$$

The ingestion rates of floodwater vary with age group, activity, and exposure duration. While Dorevitch et al. (2011) reported ingestion rates based on activity (3.5 mL/h for pedestrians), Huynh et al. (2024) refined these estimates by applying this rate for adults and 3.7 mL/h for children. The time of exposure to contaminated water is derived from the survey data collected in 2013, reflecting the time residents reported being in contact with floodwater. These points are spatially interpolated across the extension of the study area using inverse distance-based weighted interpolation (IDW), generating a continuous, spatial exposure layer of time of exposure.

A dose-response analysis is carried out for the modelled doses of the two pathogens. First, the probability of infection (P_{inf}) denotes the probability that will occur when an individual is exposed to an average ingested dose (μ) of a particular pathogen (eq. 13). Considering the probability of infection to more than one microorganism, the Beta-Poisson model is used.

$$P_{inf} = 1 - \left(\frac{\mu}{\beta}\right)^{-\alpha} \quad (13)$$

where α and β are parameters of the beta distribution, specific to each pathogen. Following the probability of infection, the probability of illness (P_{ill}) denotes the probability of developing symptoms of acute illness $(P_{ill|inf})$ after an infection (P_{inf}) calculated using Equation 14:

$$P_{ill} = P_{inf} \times P_{ill|inf} \quad (14)$$

The risk of illness is a specific parameter of each pathogen. These parameters are given in Table 1:

Table 1. Infection parameters for pathogens

Inputs	Values	Units	References
Intake rates (IR)	3.5 (children) 3.7 (adults)	mL/h	Dorevitch et al. (2011); Huynh et al. (2024)
α Rotavirus A	0.253		Haas et al. (2014)
β Rotavirus A	0.422		Haas et al. (2014)
α *E. coli**	0.373		WHO (2016)
β *E. coli**	39.71		WHO (2016)
Risk of illness given infection to Rotavirus A $(P_{ill|inf})$	0.50		WHO (2016)

https://doi.org/10.5194/egusphere-2026-850
Preprint. Discussion started: 17 February 2026

Risk of illness given infection to *E. coli* $(P_{ill\|inf})$	0.25	Iwu et al. (2022)

* The clinical data on the infectivity of *E. coli* O157:H7 to humans are not available. These parameters are presented in WHO (2016), developed from outbreaks.

2.4. Economic risk and disease burden metrics

2.4.1. Value/Population Health at Risk:

The Value at Risk (VaR) is a probabilistic estimate of the minimum loss given a specific exceedance probability. Flood losses are obtained from the product of the relative losses to buildings (*rbloss*) corresponding to an event with a return period of 100 years and current building values (*bv*) (in US$). Therefore, the VaR is estimated using Equation 15.

$$VaR = rbloss \times bv \quad (15)$$

For health impacts, the disease incidence, or number of potential cases given a specific exceedance probability of flooding, is estimated. This is a function of the probability of illness (eq. 14) and the exposed population (current), and is termed as Population Health at Risk (PHaR) as shown in Equation 16.

$$PHaR = P_{ill} \times exposed\_population \quad (16)$$

2.4.2. Expected Annual Damage/Cases

Average annual building losses across the range of return periods are estimated through the Expected Annual Damage (EAD). The EAD is an expression of flood risk, as it combines the flood hazard with the likelihood over certain periods (Dp). It equally distributes risk over time, represented by the area under the curve of flood loss vs probability as shown in Equation 17.

$$EAD = \int_0^1 D(p)\, dp \quad (17)$$

EAD is computed using the trapezoidal rule, as the loss/damage used as input is expressed as specific probabilities, and for specific return periods. The trapezoidal rule approximates the integral by connecting the damage to the given periods (p_1, D_1), (p_2, D_2), ..., (p_n, D_n) (see eq. 17). This was done for the return periods rp = 2, 5, 10, 20, 50, 100 yr. The resulting EADs were aggregated on the ward level, similarly to Scheiber et al. (2024), as shown in Equation 18.

$$\int_{p_n}^{p_1} D(p)\, dp = \sum_{i=1}^{n-1} \frac{D_i + D_{i+1}}{2} \times (p_i - p_{i+1}) \quad (18)$$

Similar to the EAD, the expected cases of illnesses related to rotavirus A and *E. coli* are estimated through the expected annual cases (EAC). It combines the probability of illnesses across all return periods with the exposed population (see sections 2.3.2 and 2.3.3).

https://doi.org/10.5194/egusphere-2026-850
Preprint. Discussion started: 17 February 2026

3. Results and Discussion

3.1. Predictive performance of flood impact models

We compared candidate Bayesian regression models for predicting residential building loss (*rbloss*) and concentrations of *E. coli* (*ecoli*) and rotavirus A (*rota*) in flood waters as described in Section 2.2. The candidate model comparison is presented in the Supplementary Material (Bayesian Regression Models in S2.1). Model m_2, which includes water depth (*wd*) and building value (*bv*) as predictors, provided the best predictive performance for building losses.

Among the models developed to predict rotavirus A and *E. coli* concentrations (see, section 2.2.2), comparative evaluation of model performance indicated that the hurdle lognormal model outperformed the other tested configurations, as it effectively captured both the binary occurrence (presence or absence) and the positive continuous concentrations (non-zero observations) of pathogens in water samples. The inclusion of additional predictors did not enhance model performance, suggesting that the intercept-only formulation provided a more parsimonious and robust representation of the observed microbial concentration patterns. The model parameters of the chosen candidate models are provided in Supplementary material (Model parameters of the chosen candidate models S2.3).

The models were trained using empirical data on relative building losses (*rbloss*), and pathogen concentrations (rotavirus A, *rota*, and *E. coli*, *ecoli*). Model evaluation followed a k-fold cross-validation (k = 10). As shown in Table 2, the *rbloss* model achieved low error metrics (*MAE* = 0.13, *MBE* = -0.02), indicating relatively strong predictive performance. However, for both the rotavirus A and *E. coli* predictions, the *MBE* is of the same order of magnitude as the *MAE*, indicating that the models struggle to accurately reproduce extreme observations, particularly high-contamination levels.

Across all cases, the *CRPS* is lower than the *MAE*, demonstrating that the probabilistic predictions are better calibrated and more accurate than deterministic point estimates. Consequently, in applying the impact models, we use the full predictive distribution to quantify uncertainty and derive the associated risk metrics.

Table 2. Predictive performance metrics of the flood impact models.

Model	MAE	RMSE	MBE	MEAN CRPS
rbloss (relative, no unit)	0.13	0.19	–0.02	0.08
rota (gc/mL)	5.43×10^6	7.73×10^6	-5.38×10^6	3.66×10^5
ecoli (CFU/mL)	7.77×10^3	1.18×10^4	-6.90×10^3	6.31×10^2

https://doi.org/10.5194/egusphere-2026-850
Preprint. Discussion started: 17 February 2026

3.2. Flood risks

3.2.1. Economic flood risk

The Value at Risk (VaR) was estimated for residential buildings in Can Tho in thousands of US dollars (1k US$) (see, section 2.4.1). The estimates reveal distinct spatial and statistical patterns across percentiles, with ward-level losses ranging from US$3.06k ($Q_{25}$) to US$10,533k (Q_{75}), with a median of US$792.02k (see, Figure 5). The total VaR for Can Tho city is between US$1,415.63k ($Q_{25}$) and US$82,840.20k (Q_{75}) with a median at US$24,304.11k.

The estimates per ward were highest in Phu Thu (PTU, Cai Rang district), with a median (Q_{25}; Q_{75}) of US$3,137.07k (189.11k; 10,532.26k), followed by Thuong Thanh (TT, Cai Raing district) and Long Tuyen (LT, Binh Thuy district), with medians (Q_{25}; Q_{75}) of US$1,995.42k (120.00k; 6,704.07k) and US$1,606.33k (93.38k; 5,499.83k), respectively.

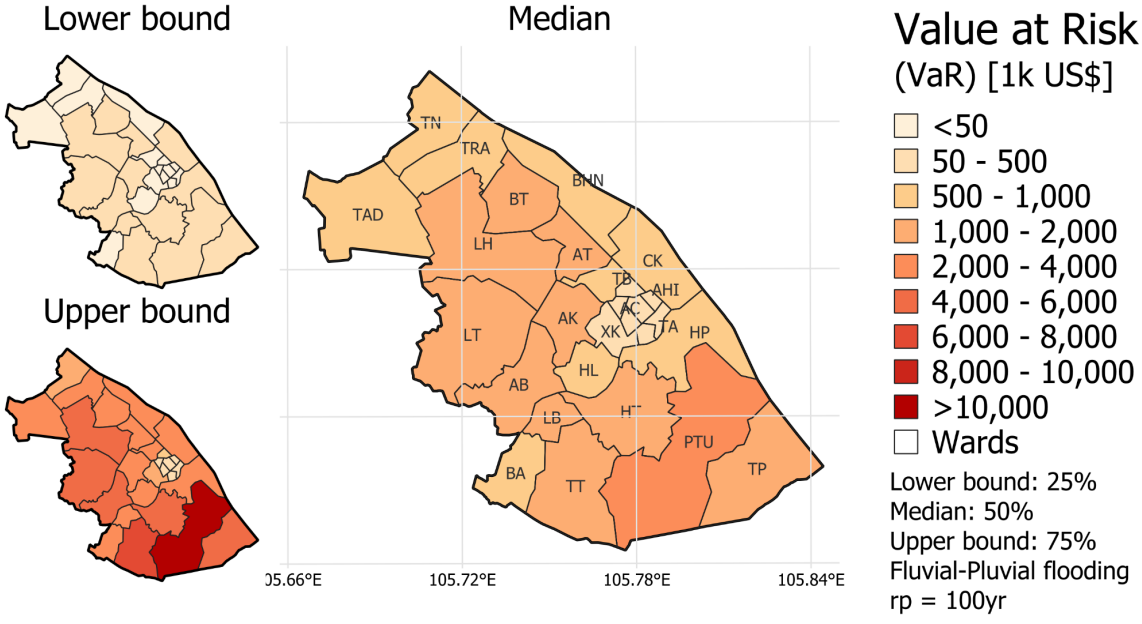

Figure 5. Value at Risk (VaR) for residential buildings at the 25th (lower bound), 50th (median), and 75th (upper bound) percentiles.

Ninh Kieu district generally exhibits the lowest building losses, whereas Cai Rang and Binh Thuy districts show the highest losses. This spatial pattern indicates inter-district variability. The observed differences in VaR estimates highlights the influence of local factors that can be attributed to diversity in building values (socio-economic attributes) and drainage capacity. We identify a strong resemblance with water depth distribution, due to the dependence of water depth as a predictor in the model, as described by Scheiber et al. (2024). As the administrative and economic core of Can Tho, Ninh Kieu concentrates governmental institutions, health facilities, and commercial services, which would explain a higher exposure of high-value buildings to flood impacts (Chinh et al., 2017). However, this district is largely protected by dykes, substantially reducing the flood hazard.

https://doi.org/10.5194/egusphere-2026-850
Preprint. Discussion started: 17 February 2026

While the Value at Risk provides an insight into potential building losses at a specific exceedance probability, the Expected Annual Damage (EAD) integrates these probabilistic losses over the return periods, capturing the recurring economic burden of flooding (see, Figure 6). The estimated EAD for Can Tho city is between US$1.33k ($Q_{25}$) and US$4,723.95k (Q_{75}) with a median at US$363.00k.

The total EAD for Can Tho was estimated at a median of US$10,683.68k, with an interquartile range (Q_{25}–Q_{75}) of US$610.36k to US$36,624.45k. Through the median (Q_{25}; Q_{75}) of EAD, the wards of Phu Thu (PTU), Thuong Thanh (TT), and An Binh (AB) displayed the highest estimated losses, with values of US$1,392.25k (81.61k; 4,723.95k), US$857.34k (49.59k; 2,906.82k), and US$673.04k (36.58k; 2,376.88k), respectively. These results indicate that Phu Thu ward in Cai Rang experiences high economic losses in the city.

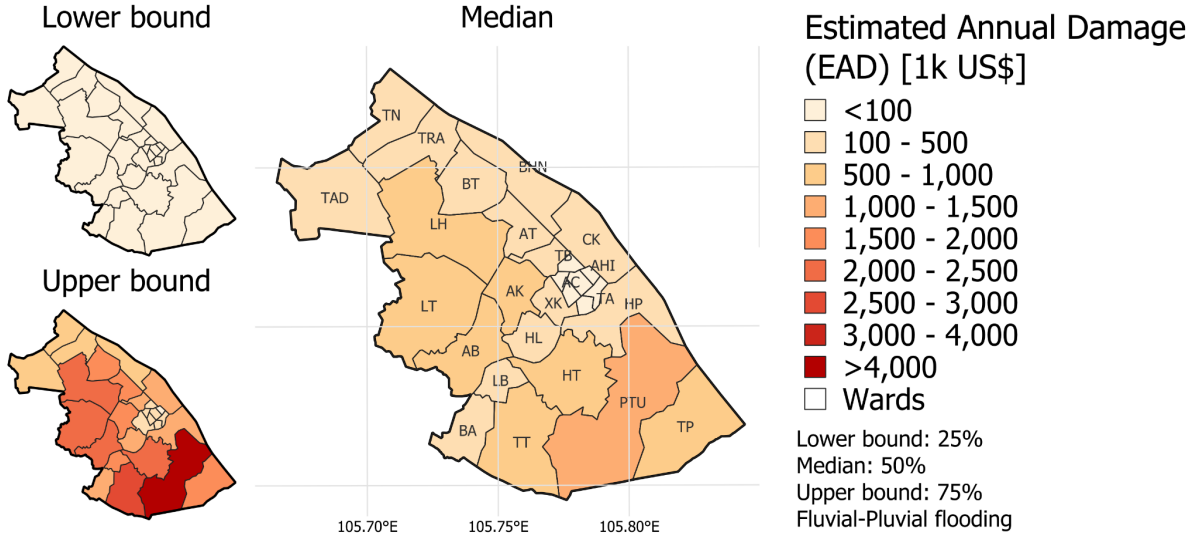

Figure 6. Expected Annual Damage (EAD) to residential buildings at the 25th (lower bound), 50th (median), and 75th (upper bound) percentiles.

3.2.2. Flood-related Disease burden

Using models that predict pathogen concentrations in floodwater and sewer water, we estimate spatial distributions of rotavirus and *E. coli* across flood-affected areas. The doses for rotavirus are higher than the doses of *E. coli* (see Table 3). These values also differ for adults and children, as children tend to ingest larger amounts of water, due to hand-mouth contact (de Man, 2014).

Table 3. Pathogen concentration, ingested doses, infection and illness probabilities due to rotavirus A and *E. coli*.

Inputs	Units	Percentile Values		
		Lower bound (0.25)	Median (0.50)	Upper bound (0.75)
Rotavirus A ingested dose (children)	gc	0.00	4.01×10^6	4.43×10^7

https://doi.org/10.5194/egusphere-2026-850
Preprint. Discussion started: 17 February 2026

Rotavirus A ingested dose (adults)	gc	0.00	3.80×10^6	4.19×10^7
E. coli ingested dose (children)	CFU	0.00	0.00	2.59×10^4
E. coli ingested dose (adults)	CFU	0.00	0.00	2.45×10^4
Infection probability to rotavirus A (children)	%	0.00	98.28	99.07
Infection probability to rotavirus A (adults)	%	0.00	98.26	99.05
Infection probability to *E. coli* (children)	%	0.00	0.00	91.09
Infection probability to *E. coli* (adults)	%	0.00	0.00	90.90
Illness probability to rotavirus A (children)	%	0.00	49.14	49.53
Illness probability to rotavirus A (adults)	%	0.00	49.13	49.53
Illness probability to *E. coli* (children)	%	0.00	0.00	22.77
Illness probability to *E. coli* (adults)	%	0.00	0.00	22.72

* Note: Results shown for a return period rp = 100 yr.

The differences in dose-response relationship influence the infection and illness probabilities for both vulnerable groups. Though the probability of infection is high for rotavirus A (>98%), the illness probability is lower (~49%). This is also the case for *E. coli*, as not every infection (estimated at ~91%) develops into an acute illness (~23%), as also highlighted by Nguyen et al. (2017). These values are comparable with those found in Huynh et al. (2024), where the infection probability to rotavirus A ranged between 96-98%, and in Tran et al. (2024), where rotavirus A was detected in 42.7% of the cases in children. They detected coinfection of *E. coli* occurred in 45.2% of rotavirus-positive cases. However, although the water samples in this study contained both pathogens, coinfection or relationships between pathogens are not considered in the QMRA, as detailed in WHO (2016).

From the illness probabilities of rotavirus A and *E. coli* and the population of children below 5 years, we obtain the number of cases of illnesses related to those pathogens across all scenarios of flood simulations. Each exposure event is assumed to be independent, with no acquired immunity after an infection (Fuhrimann *et al.*, 2017).

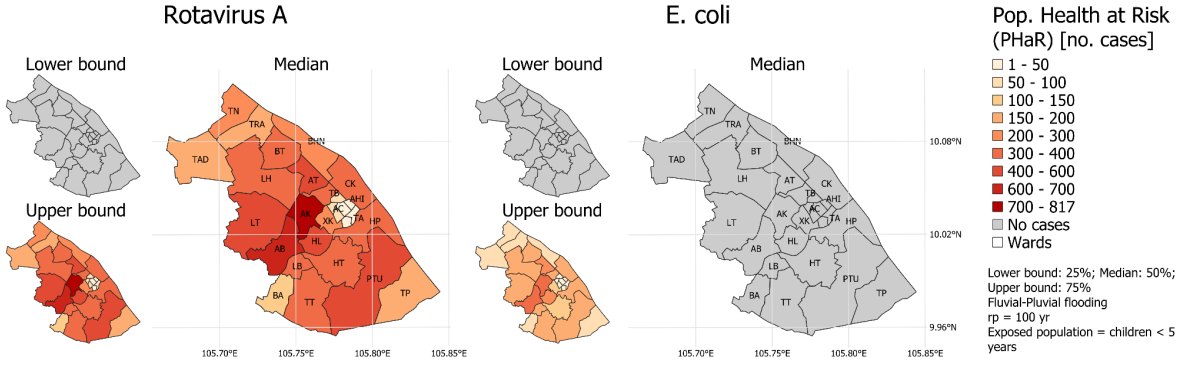

Figure 7. Population Heath at Risk (PHaR) of rotavirus A– and *E. coli*–related illness among children at the 25th (lower bound), 50th (median), and 75th (upper bound) percentiles

The PHaR represents the number of cases corresponding to a flood exceeding a 100-year event (see, Figure 7). At the ward-level, PHaR of rotavirus A is estimated at a median of 276 cases, with interquartile range (Q_{25}, Q_{75}) between 0 and 817 cases. Prevalence of cases due to *E. coli* was estimated only above the 75th percentile of the distribution. For rotavirus A, PHaR is

https://doi.org/10.5194/egusphere-2026-850
Preprint. Discussion started: 17 February 2026

the highest in wards of the district Ninh Kieu namely, An Khanh (AK), An Binh (AB), and Hung Loi (HL). For An Khanh, the cases ranged between 0 (Q_{25}) and 817 (Q_{75}), with a median of 811.

For *E. coli*, at the ward-level, the PHaR range from 0 (Q_{25}) to 377 (Q_{75}), with the maximum number of cases estimated in the ward of An Khanh (AK), followed by An Binh (AB) with 310 cases (Q_{75}), and Hung Loi (HL) with 261 estimated cases (Q_{75}). Considering the upper bound (Q_{75}), the PHaR in Can Tho City among children under 5 years of age attributable to rotavirus A and E. coli was estimated at 7,866 and 3,599 cases, respectively.

The Expected Annual Cases (EAC) is an average over the number of cases across all return periods, accounting for events with low and high impacts. Figure 8 shows the spatial distribution of EAC of rotavirus A and *E. coli* for children less than 5 years of age. At the ward-level, EAC of *E. coli* and rotavirus A is in the interquartile range of 0–185 and 0–400 cases, respectively.

EAC attributable to *E. coli* is non-zero only above the 75th percentile of the distribution. Accordingly, the Q_{75} estimate of EAC is reported at the ward-level and discussed in this section. The ward with highest EAC is An Khanh (AK) with 400 and 185 cases of rotavirus A and *E. coli*, respectively. This is followed by An Binh (AB), with 335 cases of rotavirus A and 152 cases of *E. coli*, and Hung Loi (HL), with 277 and 128 cases. With a total of 585 cases related to both rotavirus A and *E. coli* citywide, the ward of An Khanh faces the highest EAC-related disease burden.

Both pathogens cause diarrhoea, one of the most prevalent infectious diseases in Can Tho, as classified under Circular 54/2015/TT-BYT issued by the Vietnam Ministry of Health. The upper-quartile estimate (Q_{75}) of the total attributable cases (EAC) of rotavirus A and *E. coli* due solely to flooding is 3,830 cases. This value is comparable to the reported annual average of 3,541.56 cases between 2014 and 2022 (Hoang et al., 2025). However, it is to be noted that this estimate represents an upper-bound scenario and does not reflect the median disease burden.

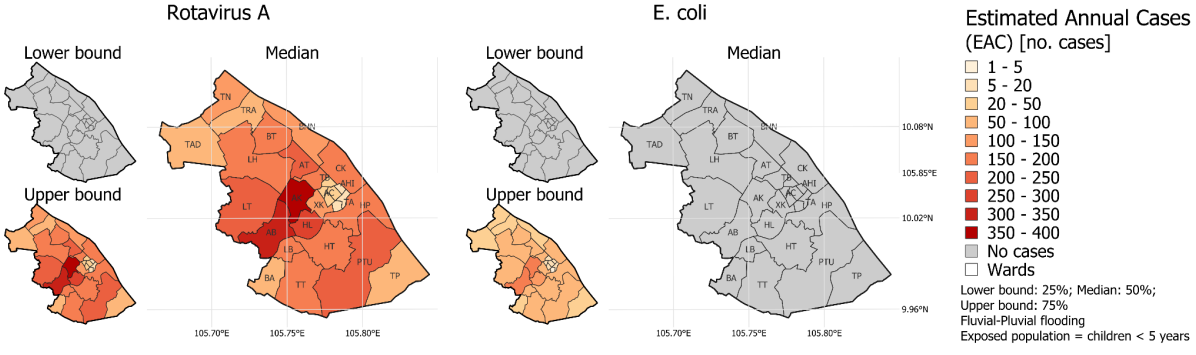

Figure 8. Expected Annual Cases (EAC) of rotavirus A– and *E. coli*–related illness among children at the 25th (lower bound), 50th (median), and 75th (upper bound) percentiles.

3.3. Intersecting Economic risk and Disease burden

The spatial intersection of economic risk and disease burden provides a comprehensive picture on the complex nature of flood risks in Can Tho. Such a multi-risk approach reveals how (socio)economic constraints and health-related exposures interact to

https://doi.org/10.5194/egusphere-2026-850
Preprint. Discussion started: 17 February 2026

intensify the consequences of flooding. Locations with high economic losses may not correspond to elevated disease burden and regions where both risks overlap represent critical points of compounded flood risk. Identifying these convergence zones is essential for disaster risk management.

Figure 9 depicts bivariate distribution maps of the spatial relationship between economic risks and disease burden in Can Tho city, using the results obtained for Expected Annual Damage (EAD) and Expected Annual Cases (EAC). The colour gradients represent the intersection of both indicators. Darker tones indicate a higher intensity of the risks, while lighter shades correspond to lower combined risk levels. The highest intersected risks for both pathogens are concentrated in Phu Thu (PTU) and Thuong Thanh (TT) wards of Cai Rang district, as well as An Binh (AB) ward in Ninh Kieu district. Rotavirus A exhibits higher combined risks, whereas *E. coli* is more weakly coupled to economic losses. Conversely, low-risk areas are consistent across both pathogens, reflecting low economic losses and low disease burden. These are located in the Ninh Kieu district, particularly in the wards of An Hoi (AH), An Lac (AL) and Tan An (TA).

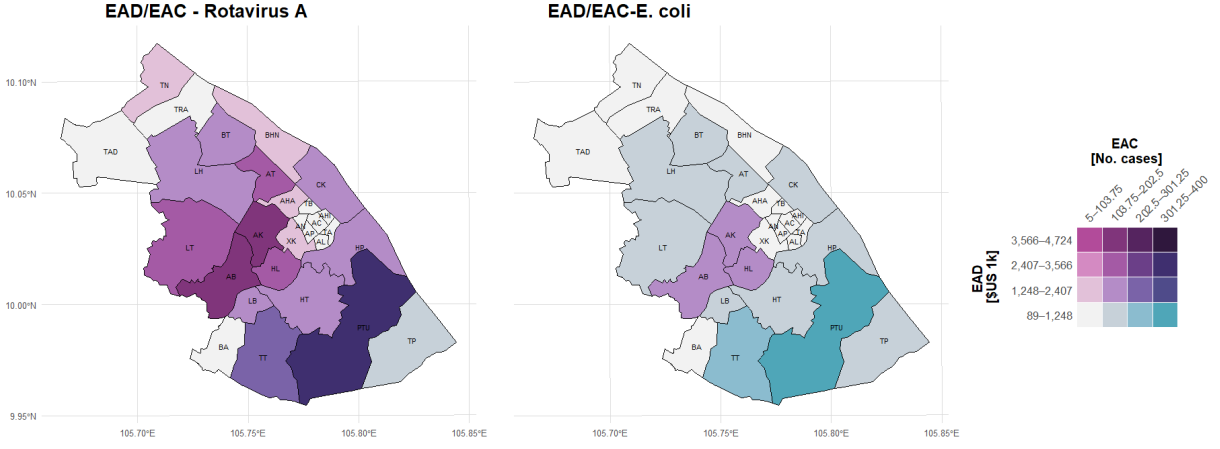

Figure 9. Bivariate choropleth map illustrating flood-related economic risk and disease burden among children under 5 years old at the 75th percentile (Q75).

Flood defence infrastructure projects have been continuously implemented in Can Tho to protect the urban core, which is primarily located in Ninh Kieu District (The World Bank, 2025). These interventions have the potential to reduce future flood risk, even though significant disparities persist between high- and low-risk areas within the same district. Our study used observations from retrospective flood events and a snapshot of flood risk reduction infrastructure (including the dyke ring). Despite having plausible results for the present scenario, the study does not address the projections and uncertainties associated with changing climate. In addition to future climatic factors, urban expansion is expected to be a major driver of flood risk (Storch & Downes, 2011). Tierolf et al. (2021) noted that in densely populated regions such as the Vietnamese Mekong Delta, ongoing urban growth is likely to increase the EAD, thereby amplifying overall flood risk. In parallel, urban development may drive the expansion and improvement of sewage and drainage infrastructure. Such advancements could contribute to lowering

https://doi.org/10.5194/egusphere-2026-850
Preprint. Discussion started: 17 February 2026

the risk of water contamination by limiting sewer overflows and enhancing wastewater management during flood events. These improvements would not only mitigate direct disease burden associated with pathogenic exposure but also strengthen urban resilience to compound flooding.

The findings from this study highlight the need to determine the extent of the interactions between flood risk, socioeconomic vulnerability, and public health, particularly in relation to economic losses and infectious disease burden. Addressing these interconnections, as highlighted by Torti (2012) presents opportunities for policy-oriented discussions about the inclusion of additional dimensions of risk in disaster risk assessments, moving beyond single-risk silos, centred in financial terms. With public health recommendations in addition to information on economic losses, our study's findings can ultimately inform and guide local responses with crucial policy implications, allowing the health sector to allocate resources efficiently and better prepare for seasonal disease surges, as well as incentivising private precautionary measures to reduce risks.

4. Conclusions

This study advances the understanding of flood risks in Can Tho, Vietnam, by integrating economic and health dimensions through the intersection of residential building losses and pathogen concentration models. The observed spatial variability in both physical and health impacts suggest heightened vulnerabilities that may reflect underlying disparities attributed to drainage system limitations, building characteristics, demographic and household socio-economic conditions. The presence of pathogens such as *E. coli* and rotavirus A in flood and sewer water highlights the public health implications of flooding, particularly for vulnerable population groups. Disaster risk reduction interventions, including the construction of flood defences and the expansion and improvement of sewage systems, have the potential to reduce the exposure to floodwater, thereby lowering economic losses and illness probabilities.

Nevertheless, with continued urban expansion and population growth, Can Tho is likely to face increasing pressures on its drainage networks in terms of coverage, interconnection, and hydraulic capacity. If unaddressed, these conditions may lead to exacerbated flood impacts, underscoring the need for integrated disaster risk management. Future research should incorporate additional explanatory variables, explore sensitivity analyses across different locations, and refine the proposed impact models to improve their robustness and transferability. Overall, the integrative framework developed in this study provides a foundation for designing comprehensive flood risk reduction strategies in flood-prone cities such as Can Tho.

https://doi.org/10.5194/egusphere-2026-850
Preprint. Discussion started: 17 February 2026

Code, data, or code and data availability

The survey data used in this research is openly available as a part of the German flood damage database, HOWAS21 (Deutsches GeoForschungsZentrum GFZ, 2011). The microbial concentration dataset is available at Hyunh et al. (2023). The building exposure dataset is available at Oostwegel et al. (2025).

Supplement link

The link to the supplement will be included by Copernicus, if applicable. (Supplement is attached)

Author contributions

YV: Conceptualization, Methodology, Formal Analysis, Writing – Original draft, Writing – Review and editing; HA: Methodology, Writing – review and editing; LJNO: Data Curation, Methodology, Writing – review and editing; TTNH: Conceptualization, Methodology, Writing – review and editing; HQN: Methodology, Writing – review and editing; NKD: Methodology, Writing – review and editing; AC: Writing – review and editing, Supervision; NS: Conceptualization, Methodology, Writing – Review and editing, Supervision

Competing interests

One of the authors is a guest editor of the SI.

Disclaimer

Copernicus Publications adds a standard disclaimer: "Copernicus Publications remains neutral with regard to jurisdictional claims made in the text, published maps, institutional affiliations, or any other geographical representation in this paper. While Copernicus Publications makes every effort to include appropriate place names, the final responsibility lies with the authors. Views expressed in the text are those of the authors and do not necessarily reflect the views of the publisher."

Please feel free to add disclaimer text at your choice, if applicable.

Acknowledgements

Yamile Villafani and Nivedita Sairam are funded by BMFTR (Bundesministerium Forschung, Technologie und Raumfahrt) Grant FKZ 01LN2209A. The survey data collection was carried out as part of the "Water related Information System for a Sustainable development of the Mekong Delta" (WISDOM II) project. We thank all respondents for participating in the survey. The water sampling activity was supported by local agencies (Can Tho Environmental Monitoring Center, Can Tho Drainage

https://doi.org/10.5194/egusphere-2026-850
Preprint. Discussion started: 17 February 2026

and Sewage Company, and Can Tho Preventive Medicine Center) and analysis of the microbial parameters were carried out by Oxford University Clinical Research Unit in Vietnam (OUCRU).

Financial support

Yamile Villafani and Nivedita Sairam are funded by BMFTR (Bundesministerium Forschung, Technologie und Raumfahrt) Grant FKZ 01LN2209A.

Review statement

The review statement will be added by Copernicus Publications listing the handling editor as well as all contributing referees according to their status anonymous or identified.

References

Anders, K. L., Thompson, C. N., Thuy, N. T. V., Nguyet, N. M., Tu, L. T. P., Dung, T. T. N., Phat, V. V., Van, N. T. H., Hieu, N. T., Tham, N. T. H., Ha, P. T. T., Lien, L. B., Chau, N. V. V., Baker, S., & Simmons, C. P. (2015). The epidemiology and aetiology of diarrhoeal disease in infancy in southern Vietnam: A birth cohort study. International Journal of Infectious Diseases, 35, 3–10. https://doi.org/10.1016/j.ijid.2015.03.013.

Apel, H., Vorogushyn, S., & Merz, B. (2022). Brief communication: Impact forecasting could substantially improve the emergency management of deadly floods: case study July 2021 floods in Germany. Natural Hazards and Earth System Sciences, 22(9), 3005–3014. https://doi.org/10.5194/nhess-22-3005-2022.

Apel, H., Martínez Trepat, O., Hung, N. N., Chinh, D. T., Merz, B., & Dung, N. V. (2016). Combined fluvial and pluvial urban flood hazard analysis: Concept development and application to Can Tho city, Mekong Delta, Vietnam. Natural Hazards and Earth System Sciences, 16(4), 941–961. https://doi.org/10.5194/nhess-16-941-2016.

Apel, H., Benisch, J., Helm, B., Vorogushyn, S., & Merz, B. (2024). Fast urban inundation simulation with RIM2D for flood risk assessment and forecasting. Frontiers in Water, 6, 1310182. https://doi.org/10.3389/frwa.2024.1310182.

Bouwer, L. M. (2019). Observed and Projected Impacts from Extreme Weather Events: Implications for Loss and Damage. In R. Mechler, L. M. Bouwer, T. Schinko, S. Surminski, & J. Linnerooth-Bayer (Eds.), Loss and Damage from Climate Change (pp. 63–82). Springer International Publishing. https://doi.org/10.1007/978-3-319-72026-5_3.

Buch, A., Paprotny, D., Rafiezadeh Shahi, K., Kreibich, H., & Sairam, N. (2025). Modelling flood losses of micro-businesses in Ho Chi Minh City, Vietnam. Natural Hazards and Earth System Sciences, 25(7), 2437–2453. https://doi.org/10.5194/nhess-25-2437-2025.

Can Tho City Statistics Office. (2018). Can Tho City Statistical Yearbook 2018. Statistical Publishing House.

https://doi.org/10.5194/egusphere-2026-850
Preprint. Discussion started: 17 February 2026

Can Tho City Statistics Office. (2025). Can Tho City Statistical Yearbook 2024. Statistical Publishing House.

Cantho Water Supply – Sewerage Joint Stock Company (CWS). (2024). Annual Report 2024. https://ctn-cantho.com.vn/uploads/news/2025_04/CTW%20-%20Annual%20Report%202024%20v3_en_Tr_final_signed.pdf.

Chinh, D., Gain, A., Dung, N., Haase, D., & Kreibich, H. (2015). Multi-Variate Analyses of Flood Loss in Can Tho City, Mekong Delta. Water, 8(1), 6. https://doi.org/10.3390/w8010006.

Chinh, D.T.; Bubeck, P.; Dung, N.V.; Kreibich, H. (2016). The 2011 flood event in the Mekong delta: Preparedness, response, damage, and recovery of private households and small businesses. Disaster, 40, 753–778.

Chinh, D., Dung, N., Gain, A., & Kreibich, H. (2017). Flood Loss Models and Risk Analysis for Private Households in Can Tho City, Vietnam. Water, 9(5), 313. https://doi.org/10.3390/w9050313.

Climate and Development Knowledge Network. (2012). Managing climate extremes and disasters in Asia: Lessons from the SREX report. https://cdkn.org/page/srex.

D'Ayala, D., Wang, K., Yan, Y., Smith, H., Massam, A., Filipova, V., & Pereira, J. J. (2020). Flood vulnerability and risk assessment of urban traditional buildings in a heritage district of Kuala Lumpur, Malaysia. Natural Hazards and Earth System Sciences, 20(8), 2221–2241. https://doi.org/10.5194/nhess-20-2221-2020.

Darnkachatarn, S., & Kajitani, Y. (2025). Flood damage assessment model of industrial sectors in a Megacity: Derivation from business survey data in the Bangkok Metropolitan Region. International Journal of Disaster Risk Reduction, 118, 105221. https://doi.org/10.1016/j.ijdrr.2025.105221.

Deutsches GeoForschungsZentrum GFZ. (2011). HOWAS 21—Hochwasserschadensdatenbank [Text/csv]. Deutsches GeoForschungsZentrum GFZ. https://doi.org/10.1594/GFZ.SDDB.HOWAS21.

De Man, H., Van Den Berg, H. H. J. L., Leenen, E. J. T. M., Schijven, J. F., Schets, F. M., Van Der Vliet, J. C., Van Knapen, F., & De Roda Husman, A. M. (2014). Quantitative assessment of infection risk from exposure to waterborne pathogens in urban floodwater. Water Research, 48, 90–99. https://doi.org/10.1016/j.watres.2013.09.022.

Dorevitch, S., Panthi, S., Huang, Y., Li, H., Michalek, A. M., Pratap, P., Wroblewski, M., Liu, L., Scheff, P. A., & Li, A. (2011). Water ingestion during water recreation. Water Research, 45(5), 2020–2028. https://doi.org/10.1016/j.watres.2010.12.006.

Dung, N.V., Merz, B., Bárdossy, A., and Apel, H. (2015). Handling uncertainty in bivariate quantile estimation – An application to flood hazard analysis in the Mekong Delta. Journal of Hydrology 527(0), 704-717. doi: http://dx.doi.org/10.1016/j.jhydrol.2015.05.033.

Dung, N.V., Merz, B., Bárdossy, A., Thang, T.D., and Apel, H. (2011). Multi-objective automatic calibration of hydrodynamic models utilizing inundation maps and gauge data. Hydrol. Earth Syst. Sci. 15(4), 1339-1354. doi: https://doi.org/10.5194/hess-15-1339-2011.

Fuhrimann, S., Nauta, M., Pham-Duc, P., Tram, N. T., Nguyen-Viet, H., Utzinger, J., Cissé, G., & Winkler, M. S. (2017). Disease burden due to gastrointestinal infections among people living along the major wastewater system in Hanoi, Vietnam. Advances in Water Resources, 108, 439–449. https://doi.org/10.1016/j.advwatres.2016.12.010.

https://doi.org/10.5194/egusphere-2026-850
Preprint. Discussion started: 17 February 2026

General Statistics Office of Vietnam (GSO). (2020). Results – The Viet Nam Population and Housing Census of 00:00 hours on 1 April 2019. UNFPA and Central Population and Housing Census Steering Committee. https://vietnam.unfpa.org/en/publications/results-2019-census-population-and-housing-viet-nam.

Gonzales-Barron, U., Kerr, M., Sheridan, J. J., & Butler, F. (2010). Count data distributions and their zero-modified equivalents as a framework for modelling microbial data with a relatively high occurrence of zero counts. International Journal of Food Microbiology, 136(3), 268–277. https://doi.org/10.1016/j.ijfoodmicro.2009.10.016.

Haas, C., Rose, J. B., & Gerba, C. P. (2014). Quantitative microbial risk assessment (2nd ed). John Wiley & Sons.

Hoang, C. Q., Huynh Nguyen, Q. P., Huynh Nguyen, T. P., Nguyen, H. T., Hoang, L. T., Vu, G. H., Kim, W.-K., & Nguyen, H. D. (2025). Identification of climate-sensitive disease incidences in Vietnam: A longitudinal retrospective analysis of infectious disease rates between 2014 and 2022. Heliyon, 11(2), e41902. https://doi.org/10.1016/j.heliyon.2025.e41902.

Huynh, T. T. N., Nguyen, H. Q., Vinh, P. V., Baker, S., & Pathirana, A. (2019). Enteric pathogens in flood-related waters in urban areas of the Vietnamese Mekong Delta: A case study of Ninh Kieu district, Can Tho city. Urban Water Journal, 16(9), 634–641. https://doi.org/10.1080/1573062X.2020.1713381.

Huynh, T. T. N., Hofstra, N., Nguyen, H. Q., Baker, S., Pathirana, A., Corzo Perez, G. A., & Zevenbergen, C. (2024). Estimating disease burden of rotavirus in floodwater through traffic in the urban areas: A case study of Can Tho city, Vietnam. Journal of Flood Risk Management, 17(1), e12955. https://doi.org/10.1111/jfr3.12955.

IPCC. (2012). Managing the risks of extreme events and disasters to advance climate change adaptation. A special report of working groups I and II of the intergovernmental panel on climate change (In Field, C.B., Barros, V., Stocker, T.F., Qin, D., Dokken, D.J., Ebi, K.L., Mastrandrea, M.D., Mach, K.J., Plattner, G-K., Allen S.K., Tignor, M., Midgley, P.M., p. 582). Cambridge University Press, USA, Cambridge, UK, and New York, NY, US.

IPCC. (2022). Climate Change 2022: Impacts, Adaptation and Vulnerability. Contribution of Working Group II to the Sixth Assessment Report of the Intergovernmental Panel on Climate Change. Cambridge University Press. https://doi.org/10.1017/9781009325844.

Iwu, C. D., Iwu-Jaja, C. J., Okoh, A. I., Otim, M. E., & Al Marzouqi, A. M. (2022). Estimating the Risk of Acute Gastrointestinal Disease Attributed to E. coli O157:H7 in Irrigation Water and Agricultural Soil: A Quantitative Microbial Risk Assessment. Sustainability, 14(3), 1878. https://doi.org/10.3390/su14031878.

Jongman, B., Ward, P. J., & Aerts, J. C. J. H. (2012). Global exposure to river and coastal flooding: Long term trends and changes. Global Environmental Change, 22(4), 823–835. https://doi.org/10.1016/j.gloenvcha.2012.07.004.

Kron, W. (2005). Flood Risk = Hazard • Values • Vulnerability. Water International, 30(1), 58–68. https://doi.org/10.1080/02508060508691837.

Lison, A., Julian, T. R., & Stadler, T. (2024). Improving inference in environmental surveillance by modeling the statistical features of digital PCR. https://doi.org/10.1101/2024.10.14.618307.

https://doi.org/10.5194/egusphere-2026-850
Preprint. Discussion started: 17 February 2026

Lloyd-Smith, J. O. (2007). Maximum Likelihood Estimation of the Negative Binomial Dispersion Parameter for Highly Overdispersed Data, with Applications to Infectious Diseases. PLoS ONE, 2(2), e180. https://doi.org/10.1371/journal.pone.0000180.

Merz, B., Kreibich, H., Schwarze, R., & Thieken, A. (2010). Review article "Assessment of economic flood damage" Natural Hazards and Earth System Sciences, 10(8), 1697–1724. https://doi.org/10.5194/nhess-10-1697-2010.

Mohor, G. S., Thieken, A. H., & Korup, O. (2021). Residential flood loss estimated from Bayesian multilevel models. Natural Hazards and Earth System Sciences, 21(5), 1599–1614. https://doi.org/10.5194/nhess-21-1599-2021.

Nguyen, H. Q., Radhakrishnan, M., Huynh, T. T. N., Baino-Salingay, M. L., Ho, L. P., Steen, P. V. D., & Pathirana, A. (2017). Water Quality Dynamics of Urban Water Bodies during Flooding in Can Tho City, Vietnam. Water, 9(4), 260. https://doi.org/10.3390/w9040260.

Olcese, G., Bates, P. D., Neal, J. C., Sampson, C. C., Wing, O. E. J., Quinn, N., Murphy-Barltrop, C. J. R., & Probyn, I. (2024). Developing a Fluvial and Pluvial Stochastic Flood Model of Southeast Asia. Water Resources Research, 60(6), e2023WR036580. https://doi.org/10.1029/2023WR036580.

Oostwegel, L. J. N., Schorlemmer, D., & Guéguen, P. (2025). From Footprints to Functions: A Comprehensive Global and Semantic Building Footprint Dataset. Scientific Data, 12(1), 1699. https://doi.org/10.1038/s41597-025-06132-z.

Resilient Cities Network, Ocean Conservancy, The Circulate Initiative, & Can Tho University. (2024). Can Tho, Vietnam: City Waste Management Profile. Resilient Cities Network (R-Cities). https://www.thecirculateinitiative.org/wp-content/uploads/City-Waste-Management-Profile-Can-Tho-Viet-Nam.pdf.

Romali, N. S., & Yusop, Z. (2021). Flood damage and risk assessment for urban area in Malaysia. Hydrology Research, 52(1), 142–159. https://doi.org/10.2166/nh.2020.121.

Scheiber, L., Sairam, N., Hoballah Jalloul, M., Rafiezadeh Shahi, K., Jordan, C., Visscher, J., Zadeh, T. E., Oostwegel, L. J. N., Schorlemmer, D., Son, N. T., Nguyen Quan, H., Schlurmann, T., Garschagen, M., & Kreibich, H. (2024). Effective Adaptation Options to Alleviate Nuisance Flooding in Coastal Megacities—Learning From Ho Chi Minh City, Vietnam. Earth's Future, 12(11), e2024EF004766. https://doi.org/10.1029/2024EF004766.

Schorlemmer, D., Oostwegel, L., Calliku, D., Lobaton, P. D. L. M., Zadeh, T. E., Lingner, L., & Rao, C. (2026). Every Building On Earth – The Global Dynamic Exposure Model. https://doi.org/10.21203/rs.3.rs-8542516/v1.

Schoppa, L., Sieg, T., Vogel, K., Zöller, G., & Kreibich, H. (2020). Probabilistic Flood Loss Models for Companies. Water Resources Research, 56(9), e2020WR027649. https://doi.org/10.1029/2020WR027649.

Shrestha, B. B., Rasmy, M., Ushiyama, T., Acierto, R. A., Kawamoto, T., Fujikane, M., Ito, H., & Shinya, T. (2024). Assessment of flood damage to agricultural crops under climate change scenarios using MRI-AGCM outputs in the Solo River basin of Indonesia. Proceedings of IAHS, 386, 127–132. https://doi.org/10.5194/piahs-386-127-2024.

Storch, H., & Downes, N. K. (2011). A scenario-based approach to assess Ho Chi Minh City's urban development strategies against the impact of climate change. Cities, 28(6), 517–526. https://doi.org/10.1016/j.cities.2011.07.002.

https://doi.org/10.5194/egusphere-2026-850
Preprint. Discussion started: 17 February 2026

Tellman, B., Sullivan, J. A., Kuhn, C., Kettner, A. J., Doyle, C. S., Brakenridge, G. R., Erickson, T. A., & Slayback, D. A. (2021). Satellite imaging reveals increased proportion of population exposed to floods. Nature, 596(7870), 80–86. https://doi.org/10.1038/s41586-021-03695-w.

The World Bank. (2025). New Infrastructure Protects Viet Nam's Mekong Delta City from Chronic Floods. https://www.worldbank.org/en/news/feature/2025/08/12/new-infrastructure-protects-viet-nam-s-mekong-delta-city-from-chronic-floods.

Tierolf, L., De Moel, H., & Van Vliet, J. (2021). Modeling urban development and its exposure to river flood risk in Southeast Asia. Computers, Environment and Urban Systems, 87, 101620. https://doi.org/10.1016/j.compenvurbsys.2021.101620.

Torti, J. (2012). Floods in Southeast Asia: A health priority. Journal of Global Health, 2(2). https://doi.org/10.7189/jogh.02.020304.

Tran, K. Q., Hoang Tuan Nguyen, H., Pham, V. H., Bui, N. Q., Kieu Anh Pham, T., Ngo, T. H., & Minh Nguyen, P. (2024). A Cross-sectional Study on the Role of Rotavirus and Microbial Co-infection in Children with Acute Diarrhea in Vietnam. Archives of Pediatric Infectious Diseases, 12(1). https://doi.org/10.5812/apid-140509.

Tran, T. L., Ritchie, E. A., & Perkins-Kirkpatrick, S. E. (2022). A 50-Year Tropical Cyclone Exposure Climatology in Southeast Asia. Journal of Geophysical Research: Atmospheres, 127(4), e2021JD036301. https://doi.org/10.1029/2021JD036301.

UNFCCC. (2012). A literature review on the Topics in the context of thematic area 2 of the Work Programme on loss and damage: A range of approaches to address loss and damage associated with the adverse effects of climate change (FCCC/SBI/2012/INF.14).

UNU-EHS & Frankfurt School of Finance & Management. (2021). Compound Flood Risk and Heat Waves in Cần Thơ – Vietnam: Executive Summary. Bonn/Frankfurt: United Nations University / Frankfurt School of Finance & Management GmbH. 25pp. Available at: https://eca-network.org/projects/vietnam.

Van Der Geest, K., De Sherbinin, A., Kienberger, S., Zommers, Z., Sitati, A., Roberts, E., & James, R. (2019). The Impacts of Climate Change on Ecosystem Services and Resulting Losses and Damages to People and Society. In R. Mechler, L. M. Bouwer, T. Schinko, S. Surminski, & J. Linnerooth-Bayer (Eds.), Loss and Damage from Climate Change (pp. 221–236). Springer International Publishing. https://doi.org/10.1007/978-3-319-72026-5_9.

WHO. (2016). Quantitative Microbial Risk Assessment: Application for Water Safety Management. World Health Organization (WHO).

Win, S., Zin, W. W., Kawasaki, A., & San, Z. M. L. T. (2018). Establishment of flood damage function models: A case study in the Bago River Basin, Myanmar. International Journal of Disaster Risk Reduction, 28, 688–700. https://doi.org/10.1016/j.ijdrr.2018.01.030.

Yepes-Estrada, C., Calderon, A., Costa, C., Crowley, H., Dabbeek, J., Hoyos, M. C., Martins, L., Paul, N., Rao, A., & Silva, V. (2023). Global building exposure model for earthquake risk assessment. Earthquake Spectra, 39(4), 2212–2235. https://doi.org/10.1177/87552930231194048.

https://doi.org/10.5194/egusphere-2026-850
Preprint. Discussion started: 17 February 2026

Yirga, A. A., Melesse, S. F., Mwambi, H. G., & Ayele, D. G. (2020). Negative binomial mixed models for analyzing longitudinal CD4 count data. Scientific Reports, 10(1), 16742. https://doi.org/10.1038/s41598-020-73883-7.